variation in amplitude for the cascade realisation is larger than that for the full wave active realisation. The variation in group delay is a little larger for the wave active realisation, but not alarmingly so.

Further work, and conclusion: The lattice sections described here are most useful as non-all-pass sections, where the ability to change both amplitude and phase for a filter can be exploited to full advantage. We note that even though a non-all-pass lattice affects the amplitude, the S' and S'' blocks remain all-pass. The simulation of lattice sections in integrated filters allows the realisation of filters not previously implemented, e.g. the example filter in Reference 5.

This Letter has introduced the CMWA simulation of LC lattice sections. It has been demonstrated for a specific example that the amplitude variation for a full wave active simulation of a phase equaliser is less than for an equivalent cascade realisation. The sections introduced here are a step towards the design of integrated continuous time filters with good phase response without the use of cascade topologies.

Acknowledgment: J. Tingleff is supported financially by the Danish Technical Research Council, whose help is gratefully acknowledged.

19th January 1993

J. Tingleff and C. Toumazou (*Department of Electrical and Electronic Engineering, Imperial College, London, United Kingdom*)

References

1 TINGLEFF, J., and TOUMAZOU, C.: 'Current mode continuous time wave active filters', *Electron. Lett.*, 1992, **28**, (5), pp. 463–464

2 TINGLEFF, J., and TOUMAZOU, C.: 'CMOS integrated current mode wave active filters'. Proc. Mid-West Symp. Circuits and Systems, IEEE, 1992

3 FETTWEIS, A.: 'Wave digital filters: Theory and practice', *Proc. IEEE.*, February 1986, **74**, (2)

4 TOUMAZOU, C., LIDGEY, F. J., and HAIGH, D. G. (Eds.): 'Analogue IC design: the current-mode approach' (Peter Peregrinus Ltd., London, 1990)

5 BENNET, B. J.: 'A new filter synthesis technique—the hourglass', *IEEE Trans.*, 1988, **CAS-35**, (12), pp. 1469–1477

687

OPTICAL IN-FIBRE GRATING HIGH PRESSURE SENSOR

M. G. Xu, L. Reekie, Y. T. Chow and J. P. Dakin

Indexing terms: Optical fibres, Optical sensors

A high pressure fibre optic sensor using an in-fibre grating has been constructed. The wavelength of peak reflection from an in-fibre grating is tracked as it is pressurised, and a wavelength shift of 0·22 nm at 70 MPa hydraulic pressure has been observed. This sensor is expected to be an attractive choice for ultrahigh-pressure monitoring.

Introduction: Fibre optical Bragg grating sensors have been reported for the measurement of both temperature and strain [1]. Very important aspects of sensors based on gratings are their simplicity, small size and the relative ease and convenience in monitoring a number of sensing elements formed in a single length of fibre [2]. They are usually interrogated in the spectral domain, and therefore sensing systems based on them are relatively immune to changes in transmission of the fibre network. We report the first optical in-fibre-grating pressure sensor and results for the pressure and temperature response. We then compare the pressure and temperature sensitivity of the sensor with that theoretically expected and also with that recently achieved with a hollow-microsphere pressure sensor [3].

Our in-fibre grating pressure sensor is shown in Fig. 1. Light from a 1550 nm fibre-pigtailed ELED is coupled, via a

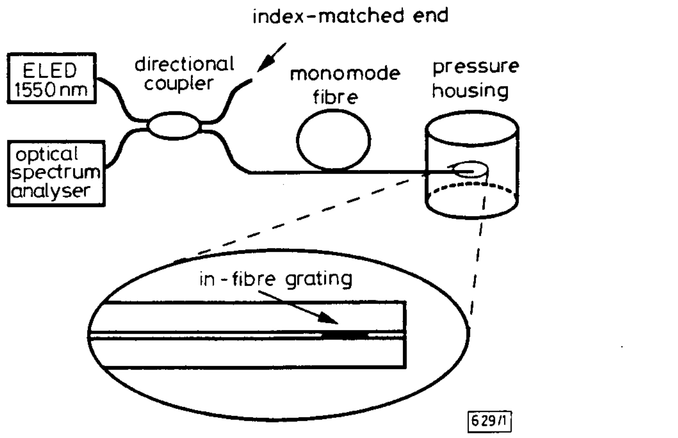

Fig. 1 *Schematic diagram of in-fibre grating pressure sensor*

directional fibre coupler, into the sensor head, which is simply a monomode fibre with an in-fibre grating. This photorefractive grating was written holographically with UV light and had a peak reflectivity of 80%, and a bandwidth of 0·7 nm at a wavelength of 1533·3 nm. The sensing probe was installed within a cavity in a high pressure vessel. When the probe was pressurised its reflectance was monitored using a commercial optical spectrum analyser (ANDO AQ-6310B), located to receive light from a return port of the coupler. Undesirable reflection from the unused output port of the coupler was suppressed using index-matching oil, whereas that from the end of the fibre with the grating was suppressed by immersion in the hydraulic oil itself. The pressure system consisted of a hydraulic pump, a commercial precision pressure transmitter (Druck PDCR 960) and a purpose-designed pressure vessel, capable of being used up to 70 MPa.

Sensitivity and discussion: When the fibre is compressed, the fractional change $\Delta\lambda_g/\lambda_g$, induced in the Bragg wavelength λ_g, in response to a pressure change ΔP, is given by

$$\frac{\Delta\lambda_g}{\lambda_g} = \frac{\Delta(n\Lambda)}{n\Lambda} = \left[\frac{1}{\Lambda}\frac{\partial\Lambda}{\partial P} + \frac{1}{n}\frac{\partial n}{\partial P}\right]\Delta P \tag{1}$$

where Λ is the spatial period of the grating and n is the effective refractive index of the fibre core. The fractional change in physical length of the fibre and refractive index of the fibre core, respectively, are given by [4]

$$\frac{\Delta L}{L} = -\frac{(1-2\mu)P}{E} \tag{2}$$

$$\frac{\Delta n}{n} = \frac{n^2 P}{2E}(1-2\mu)(2p_{12} + p_{11}) \tag{3}$$

where E and μ are the Young modulus and Poisson ratio of the fibre, respectively, and p_{11} and p_{12} are components of the strain-optic tensor. We have assumed that the fibre is mechanically homogeneous. As the fractional change in the spatial period of the grating equals the fractional change in physical length of the sensing section, the pressure sensitivity is then expected to be

$$\frac{\Delta\lambda_g}{\lambda_g\,\Delta P} = -\frac{(1-2\mu)}{E} + \frac{n^2}{2E}(1-2\mu)(2p_{12} + P_{11}) \tag{4}$$

Using a value of $7 \times 10^{10}\,\mathrm{N/m^2}$ for the Young modulus, Poisson ratio value of 0·17, values of 0·121 and 0·270 for p_{11} and p_{12}, respectively, for fused silica and a value of 1·465 for the refractive index of the germania-doped core, the predicted fractional wavelength shift is $-5{\cdot}18 \times 10^{-6}$/MPa. In fact, our measured fractional change (see Fig. 2) was $-1{\cdot}98 \times 10^{-6}$/MPa. As the values of E, μ, p_{11} and p_{12} are likely to be significantly different for the germania-doped silica glass of which the fibre core is composed, we would expect that the most likely reason for the discrepancy is our lack of knowledge of the precise values for the Young modulus, Poisson

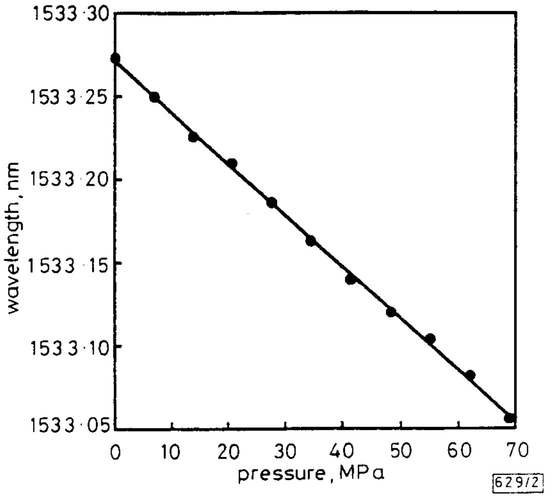

Fig. 2 *Pressure response of sensor*
λ (nm) = $-0{\cdot}0031P$ (MPa) + 1533·27
● measurements
——— linear fit

ratio and the strain-optic coefficients for the fibre core material. The cross-sensitivity to a change in temperature ΔT is expected to be

$$\frac{\Delta\lambda_g}{\lambda_g} = \left[\frac{1}{\Lambda}\frac{\partial\Lambda}{\partial T} + \frac{1}{n}\frac{\partial n}{\partial T}\right]\Delta T = (\alpha + \xi)\,\Delta T \tag{5}$$

where α is the thermal expansion coefficient of the fibre. The effects of fibre diameter change are assumed to be negligible. For our germania-doped fibre core, α is expected to be $\sim 1{\cdot}1 \times 10^{-6}$/°C. ξ is the thermo-optic coefficient, which has a value of $\sim 8{\cdot}3 \times 10^{-6}$/°C for germania-doped silica [5]. Therefore we would expect that the cross-sensitivity to temperature of the in-fibre grating is $9{\cdot}4 \times 10^{-6}$/°C. The measured figure (see Fig. 3) was $6{\cdot}72 \times 10^{-6}$/°C, or 0·01045 nm/°C. Thus our expected cross-sensitivity to temperature matches reasonably well with that experimentally observed.

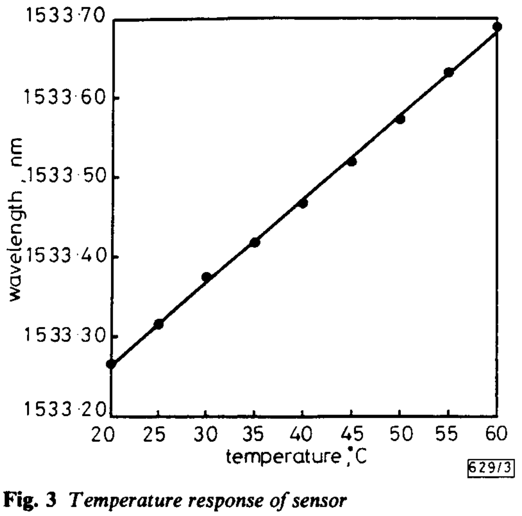

Fig. 3 *Temperature response of sensor*

Finally it is interesting to compare the sensitivity of a solid body, such as this fibre-grating sensing element, with that of a hollow type, such as the hollow microsphere type reported earlier [3]. As the mechanical compliance of solid bodies is much lower than that of hollow ones, the fractional change in wavelength with pressure is expected to be much lower for the grating sensor. In fact, the sensitivity of the in-fibre grating with pressure is actually two orders of magnitude lower than we have measured with the hollow microsphere pressure sensor under similar conditions. The ratio of the pressure sensitivity to temperature sensitivity for the in-fibre grating sensor was two orders of magnitude worse than for our microsphere type, therefore far more compensation is necessary to correct for temperature changes in the grating type. However, the grating sensor has a distinct advantage for ultrahigh pressure measurement, as it should be capable of withstanding enormous hydrostatic pressure, far in excess of that possible with the hollow sphere sensor (The hollow sphere withstood 7 MPa), and well above the range covered in these first measurements.

Conclusions: We have described a simple in-fibre grating sensor for monitoring hydrostatic pressure. A Bragg wavelength shift of $3{\cdot}04 \times 10^{-3}$ nm/MPa was observed, which is two orders of magnitude lower than we have measured with a hollow microsphere pressure sensor under similar conditions. However, this new sensor is expected to be an attractive, simple and robust miniature sensor for measuring ultrahigh pressure.

Acknowledgments: The ORC is a UK government funded (SERC) Interdisciplinary Research Centre. M. G. Xu acknowledges support under a Sino-British Friendship Scholarship.

13th January 1993

M. G. Xu, L. Reekie, Y. T. Chow and J. P. Dakin (*Optoelectronics Research Centre, University of Southampton, Southampton SO9 5NH, United Kingdom*)

References

1 MOREY, W. W., MELTZ, G., and GLENN, W. H.: 'Fibre optic Bragg grating sensors'. Proc. SPIE, 1989, **1169**, pp. 98–107
2 MOREY, W. W.: 'Distributed fibre grating sensors'. Proc. OFS '92, Monterey, USA, 1992, pp. 285–288
3 XU, M. G., and DAKIN, J. P.: 'A novel hollow-glass microsphere sensor for monitoring high hydrostatic pressure'. Proc. SPIE, O/E Fiber '92, Boston, USA, Conference Track 'Fiber Optic and Laser Sensors X', SPIE, **1795**, paper 2
4 HOCKER, G. B.: 'Fibre-optic sensing of pressure and temperature', *Appl. Opt.*, 1979, **18**, pp. 1445–1448
5 TAKAHASHI, S., and SHIBATA, S.: 'Thermal variation of attenuation for optical fibres', *J. Non-crystalline Solids*, 1979, **30**, pp. 359–370

FABRICATION OF LOW LOSS POLYMER WAVEGUIDES USING INJECTION MOULDING TECHNOLOGY

A. Neyer, T. Knoche and L. Müller

Indexing terms: Optical waveguides, Integrated optics

Singlemode polymer waveguides with low transmission loss at 1300 nm are fabricated by using injection moulding as low cost mass replication technology for the fabrication of polymer waveguide substrates. The waveguide pattern is incorporated in the substrates in the form of grooves which are filled by fully deuterated EGDMA. First buried singlemode waveguides have been realised with a transmission loss as low as 0·3 dB/cm at 1300 nm.

Introduction: One of the biggest hurdles for a wider penetration of integrated optics into the field of telecommunications and sensors is the high cost of fibre coupled and packaged devices. Until now, more than half of the costs of commercially available integrated optical components have been due to fibre coupling and packaging. Therefore new technologies are required which have the capability of low cost waveguide fabrication combined with the potential of integrating fibre alignment grooves and further alignment structures for electronic or optoelectronic components. One promising approach is the silica-on-silicon technology [1] which has shown very good loss figures and excellent thermal stability. However, the deposition of thick SiO_2 buffer layers (typ. 10 μm) and the plasma etching of thick silica waveguide layers (typ. 8 μm required for low loss, low NA waveguides at 1300 nm wavelength) with low sidewall roughness are time